托卡马克（新）经典撕裂模控制研究

张 洋

中国科学院等离子体物理研究所

中国科学技术大学，合肥　　2025年7月12日

报告提纲

- □ 背景介绍
- □ EAST新经典撕裂模控制研究
  - ➢ 控制技术、实验研究、模拟计算
- □ AI带来的变革与突破

低阶撕裂模是引发大破裂的主要物理机制

- 高密度运行区，由电流密度梯度驱动的**经典撕裂模**（TM）
- 高比压运行区，由压强梯度驱动的**新经典撕裂模**（NTM）

→ 磁岛

电阻性MHD不稳定性 —小磁岛 / 增强输运→ 降低约束限制参数 nτT —大磁岛 / 耦合、增长→ 大破裂

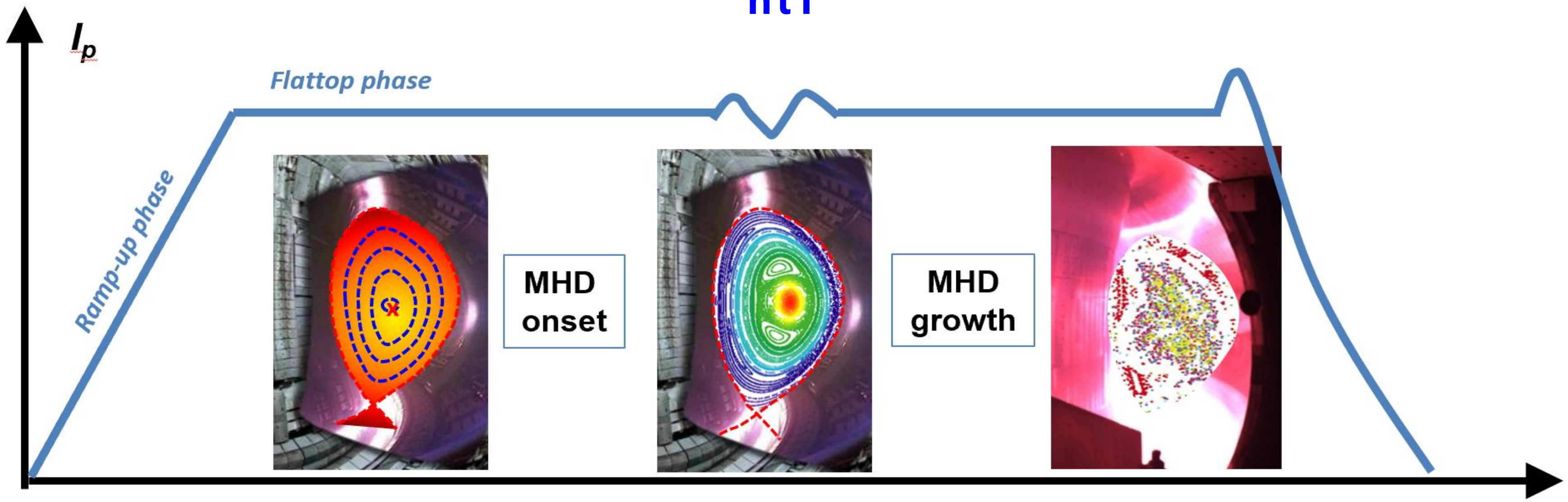

控制TM/NTM，提高约束性能，拓展运行区，避免大破裂

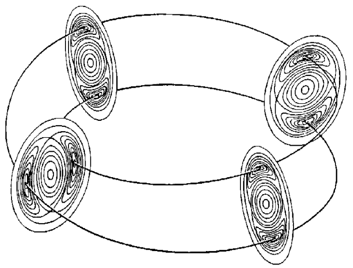

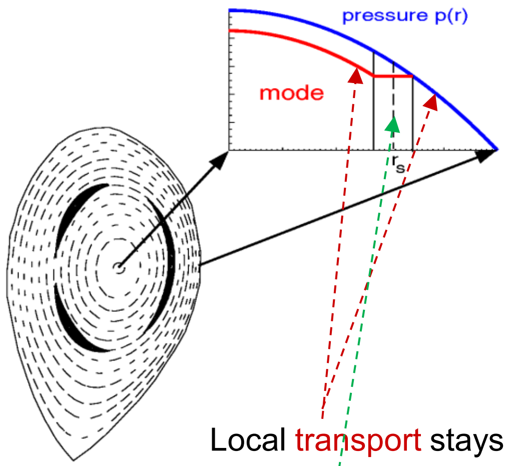

Local transport stays same outside island
But "short-circuit" across island

- 3/2-模， 降低10- 20%
- 2/1-模， 降低30-40%，容易锁模

电子回旋波是控制撕裂模的有效手段

- **电子回旋波具有局域沉积的优点，是目前已知控制磁岛的最佳手段，也是ITER的首选方案**
  - **技术难点：波束与磁岛精准（1-2 cm），快速对齐 (~100 ms)；动态变化，实时反馈**
  - **科学挑战：未来聚变堆功率需求高，如何提高控制效率?**

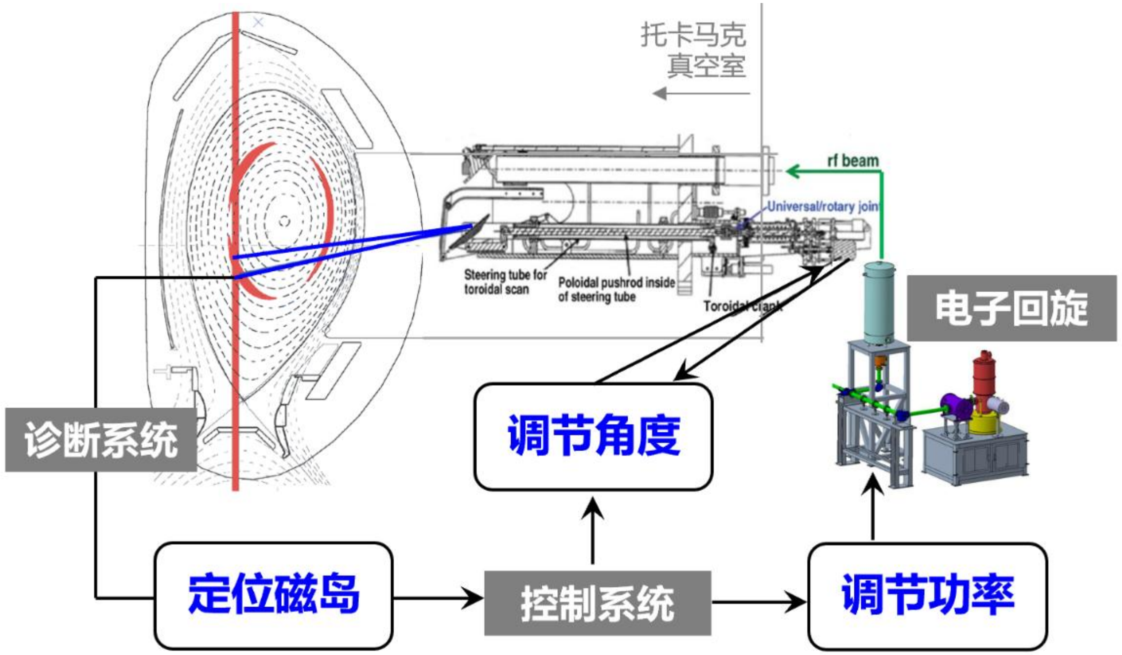

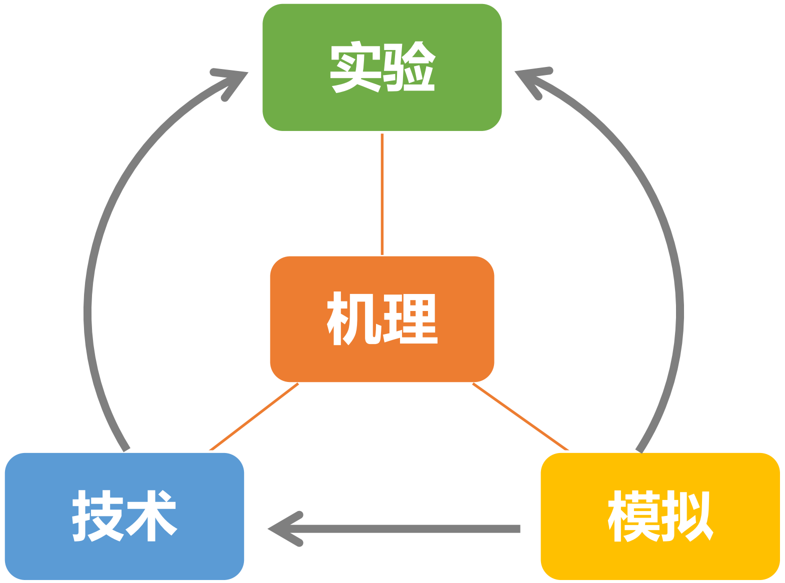

电子回旋波加热与电流驱动

- 电子回旋共振加热，共振电子吸收，经碰撞加热其它电子
- 电子回旋电流驱动： Fisch-Boozer电流模型和Ohkawa电流模型

n²>0, 波可以在等离子体中传播；n=0,截止； n=∞，共振

共振吸收频率：

$$\omega = \frac{h\Omega_{eo}}{\gamma} - k_{\|} v_{\|} \qquad \gamma \equiv [1 - v_{\|}^2/c^2 - v_{\perp}^2/c^2]^{-1/2}$$

Doppler shift（$k_{\|} v_{\|}$）；Relativistic shift（γ）

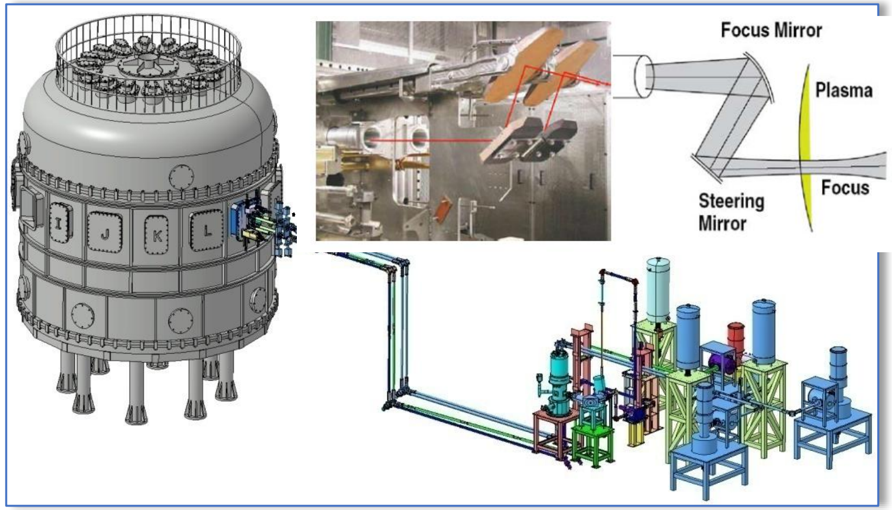

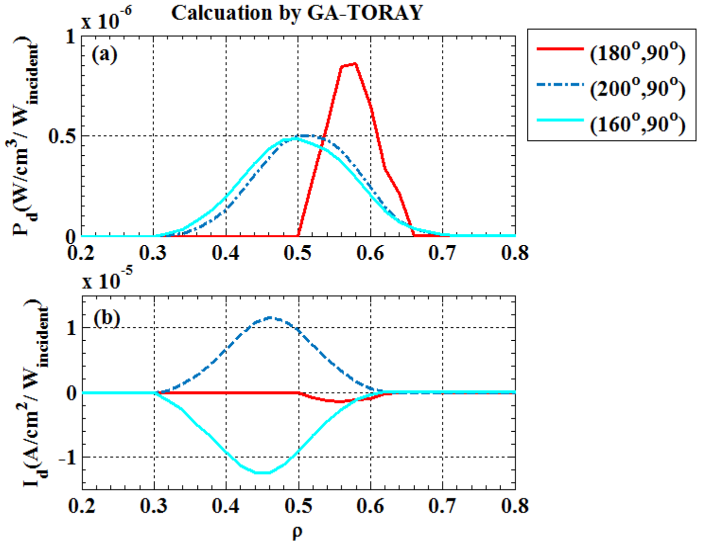

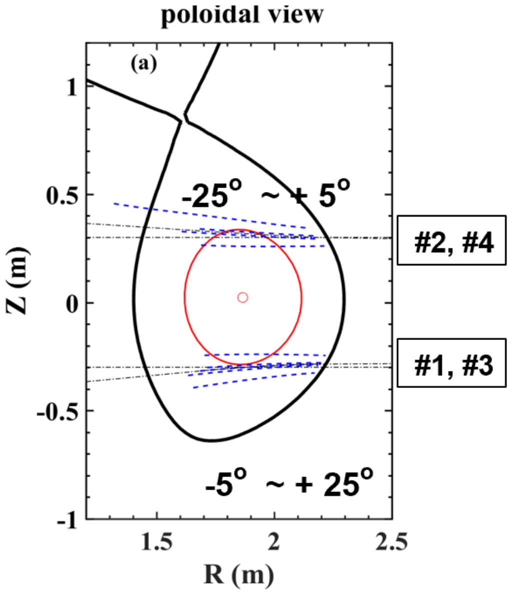

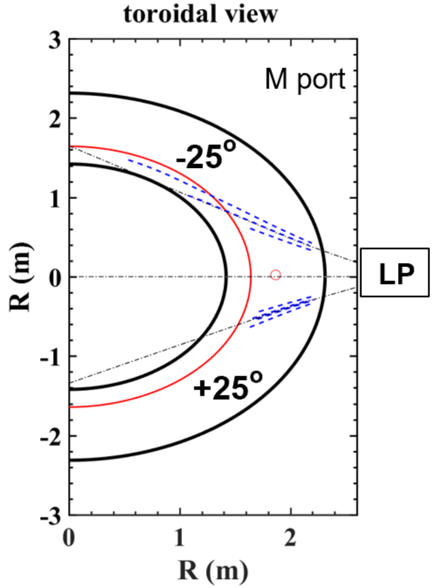

电子回旋波控制撕裂模的机理

- 撕裂模不稳定性的动理学特性可以用Modified Rutherford方程简单描述

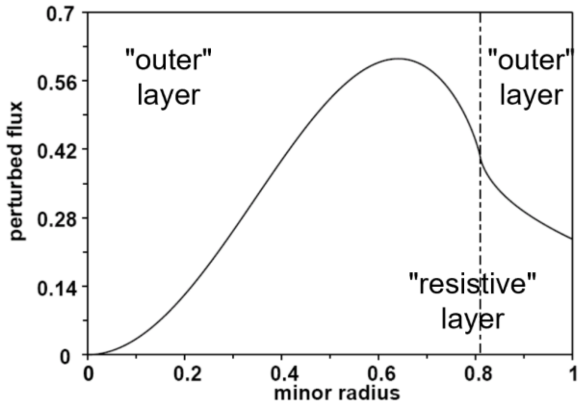

$$\Delta_0' = \frac{\psi_1'(r_+) - \psi_1'(r_-)}{\psi_1(r_s)}$$

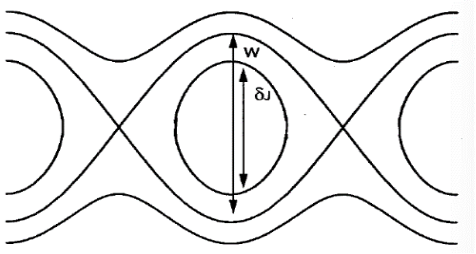

$$\frac{\tau_R}{r^2}\frac{dw}{dt} = \Delta'(w) + \varepsilon^{1/2}\frac{L_q}{L_p}\beta_p\left[\frac{w}{w^2+w_d^2} - \frac{w_{pol}^2}{w^3}\right]$$

for small ∇p, current gradient (Δ′) dominates ⇒ 'classical Tearing Mode', current driven

for larger ∇p, pressure gradient dominates: ⇒ 'neoclassical Tearing Mode', pressure driven

$$j_{bs} = -c_b\frac{\sqrt{\varepsilon}}{B_\theta}\frac{\partial p}{\partial r}$$

MRE solver for NTM dynamic

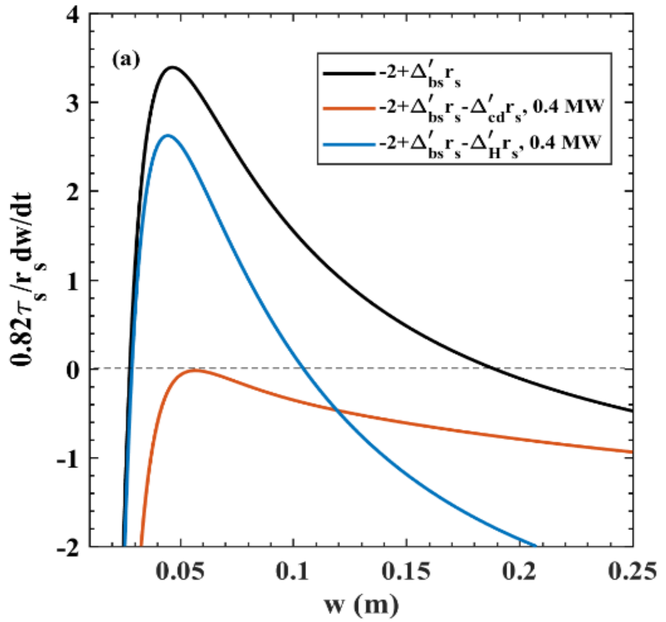

$$\Delta_{bs}' r_s \approx \varepsilon^{1/2}\frac{L_q}{L_p}\beta_p\left[\frac{w}{w^2+w_d^2} - \frac{w_{pol}^2}{w^3}\right]$$

电子回旋波控制撕裂模的机理

- 撕裂模不稳定性的动理学特性可以用Modified Rutherford方程简单描述
- 电子回旋波共振加热/电流驱动，修改电流分布，或弥补磁岛内“丢失的电流”→ 消除驱动源

$$\frac{\tau_R}{r^2}\frac{dw}{dt} = \Delta'(w) + \varepsilon^{1/2}\frac{L_q}{L_p}\beta_p[\frac{w}{w^2+w_d^2} - \frac{w_{pol}^2}{w^3}] - \Delta'_{cd} r_s - \Delta'_H r_s$$

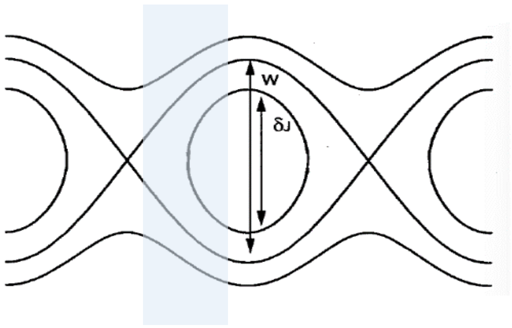

$$\frac{dT_e}{d\Omega} = -\frac{W^2}{32}\frac{\int_{-1}^{\Omega} d\Omega' \oint d\alpha \frac{S(\Omega,\alpha)}{\sqrt{\Omega'+\cos(m\alpha)}}}{\oint d\alpha\, n\chi_\perp \sqrt{\Omega'+\cos(m\alpha)}},$$

$$\eta_{\mathrm{aux}} = \frac{\int d\rho \oint \frac{d\alpha}{2\pi}\cos(m\alpha)\langle J_{\mathrm{aux}}\rangle}{\int d\rho \oint \frac{d\alpha}{2\pi}\langle J_{\mathrm{aux}}\rangle}$$

Externally driven current j_{cd} replaces the loss of current inside mangetic island, $j_{cd} / j_{bs} \sim 1.2$

Local heating changes equilibrium and local current density profile *j*(r)

$$\delta J_\parallel = \frac{3}{2}\frac{\delta T_e}{T_{e0}} J_{\parallel 0}$$

MRE solver for NTM dynamic

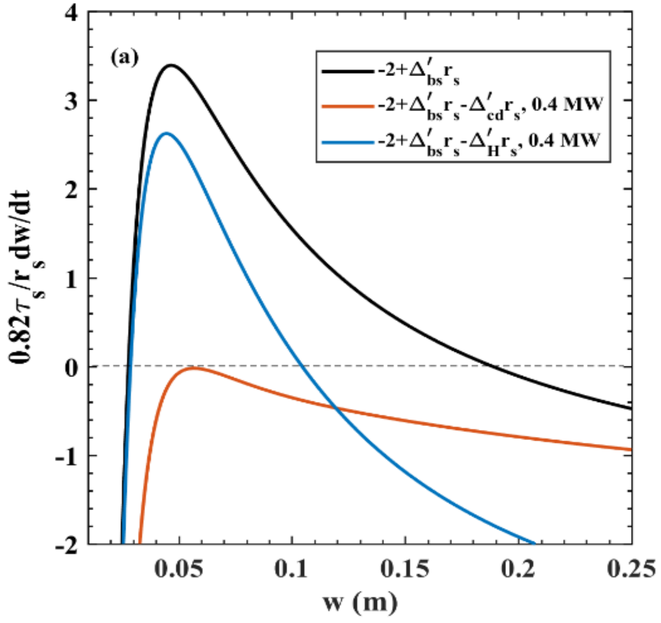

$$\Delta'_{bs} r_s \approx \varepsilon^{1/2}\frac{L_q}{L_p}\beta_p[\frac{w}{w^2+w_d^2} - \frac{w_{pol}^2}{w^3}]$$

C. C. Hegna and J. D. Callen, Phys. Plasmas 4 1997

电子回旋波控制撕裂模的方法与策略

□ 有效控制的关键是电子回旋波束与磁岛在径向位置上准确对齐

- **径向偏差**：> +/- 1 cm，效率下降60%
- **波束宽度**：磁岛减小；湍流，快电子输运展宽

  NF **55** 013023; NF **55** 033016; PRL **120**, 105001; NF **62** 066007
- **注入方式**： 连续ECCD注入，调制ECCD注入
- **注入时机**：预先注入 ECCD（小磁岛）

物理上的有效性 ⟷ 技术上的可行性

MRE @ q=m/n, neglecting curvature

$$1.22^{-1}\frac{\tau_R}{r_s}\frac{dw}{dt} = \Delta_0' r_s + 3\frac{j_{boot}}{\langle j_{||}\rangle}\frac{L_q}{r_s}\left[\frac{1}{(w/r_s)} - \frac{(3\,\varepsilon^{1/2}\rho_{\theta i}/r_s)^2}{3\,(w/r_s)^3} - K_1\frac{j_{eccd}}{j_{boot}}\frac{1}{(w/r_s)}\right]$$

Small island stabilization

Assumed <0

NTM term >0

ECCD stabilization

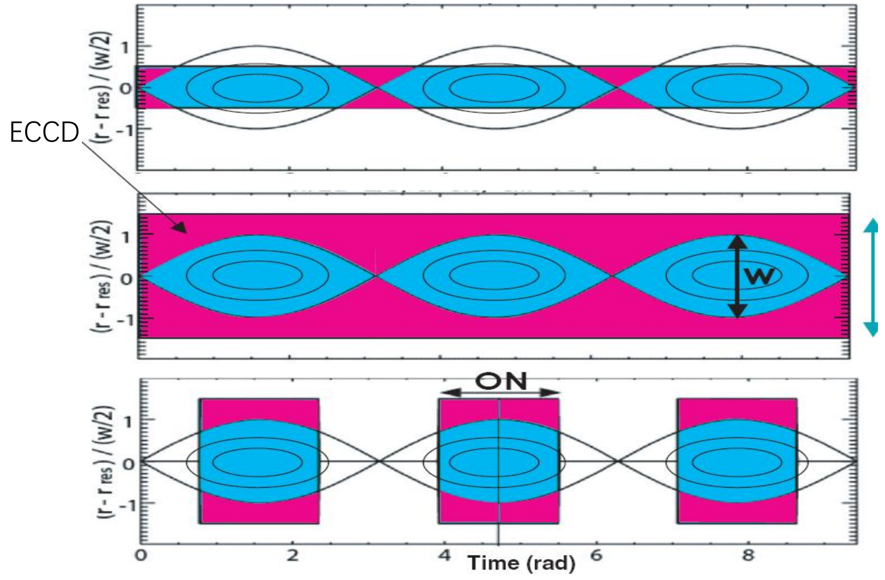

H. Zohm et al. NF 39 (1999);
M. Maraschek, et al., PRL 98 (2007)

报告提纲

- □ 背景介绍
- □ EAST新经典撕裂模控制研究
  - ➢ 控制技术、实验研究、模拟计算
- □ AI带来的变革与突破

MHD诊断系统介绍

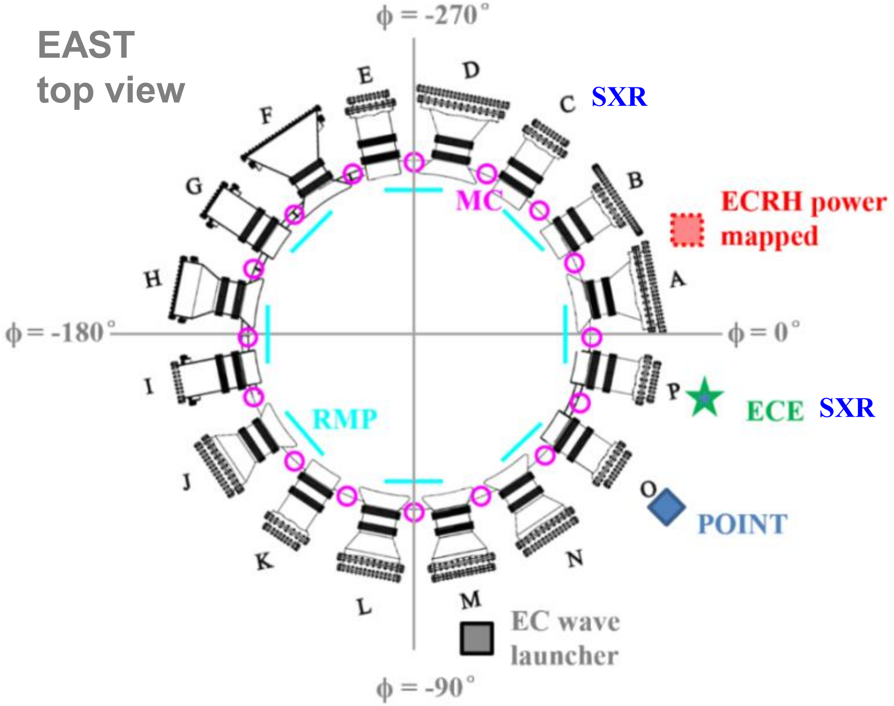

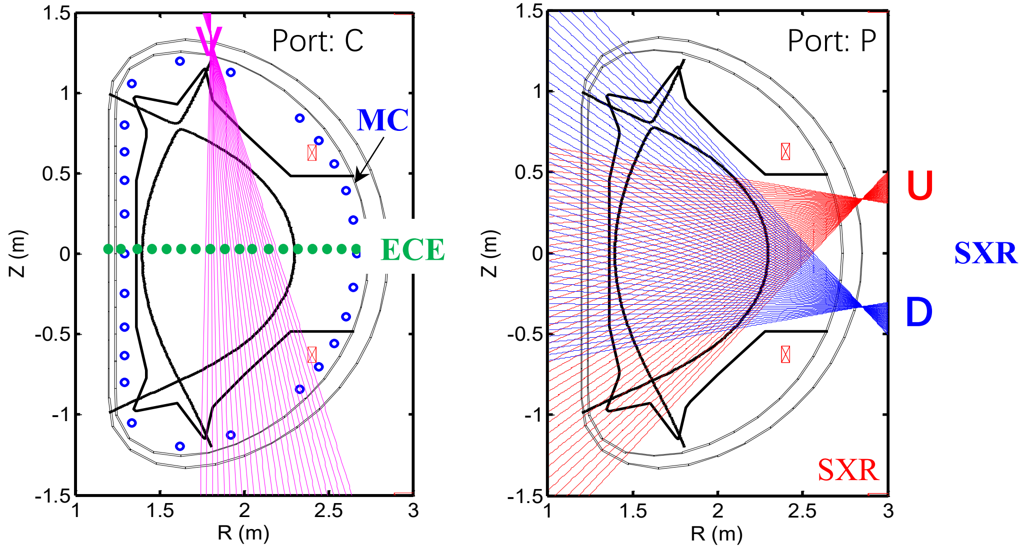

EAST shot #79810

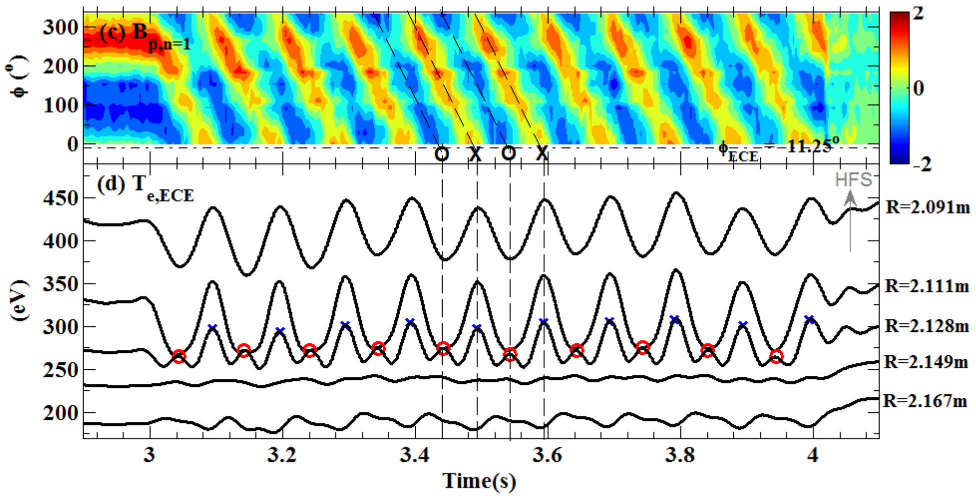

Diagnostic	Component	Spatial resolution	Time resolution
Mirnov 磁探针	8 saddle coils	~	0.5 ms
	16 Mirnov coils	~	0.02 ms
	2* 26 Mirnov coils	~	0.02 ms
电子回旋辐射（ECE）	48 channels	1 - 2 cm	10 μs
软X射线诊断（SXR）	2 arrays * 46 channels	2.5 cm	10 μs
	1 array* 24 channels		

发展新经典撕裂模主动控制技术

□ 自主研发新经典撕裂模控制技术，实现磁岛实时探测与定位追踪，研制高精度、快响应发射转镜控制机构

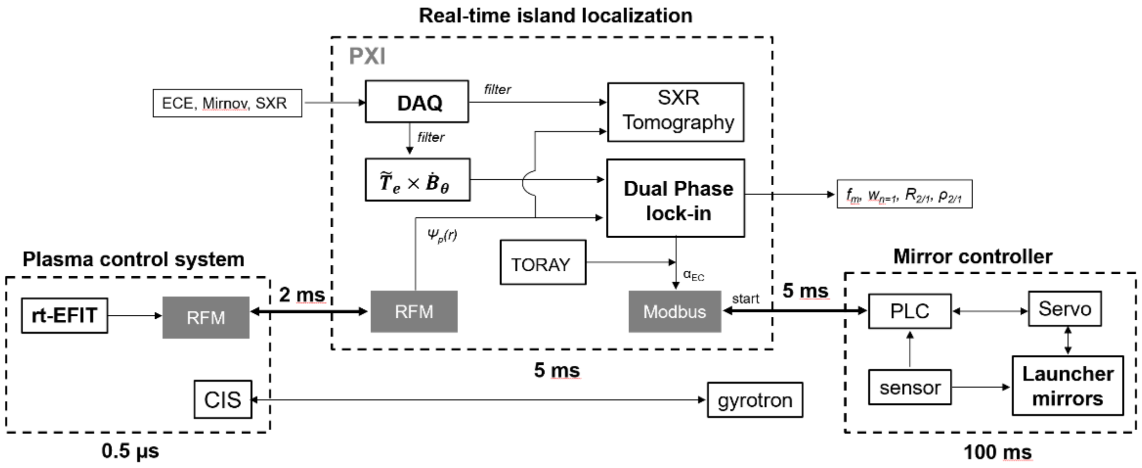

自主研发磁岛探测与实时定位追踪诊断系统

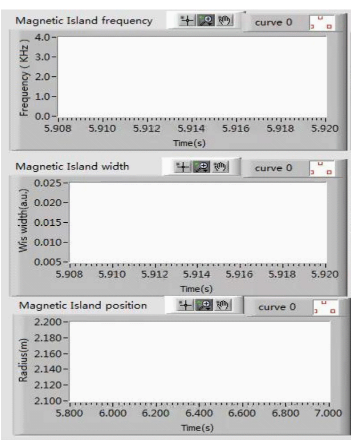

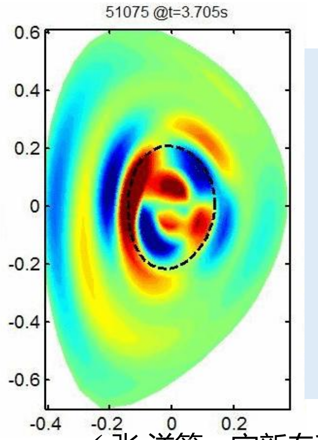

解决LHW条件下磁岛实时定位难题，实现精度1-2cm，时间分辨10ms，达到国际同等水平；目前已成为常规运行系统

✓ 张洋等，实新专利ZL201821127862，已授权，2018.7；

自主研发高精度、快响应电机运动控制机构实现波束调节

解决大负载电机微行程的瞬时启停问题，实现0.5°/50ms，达到国际先进水平

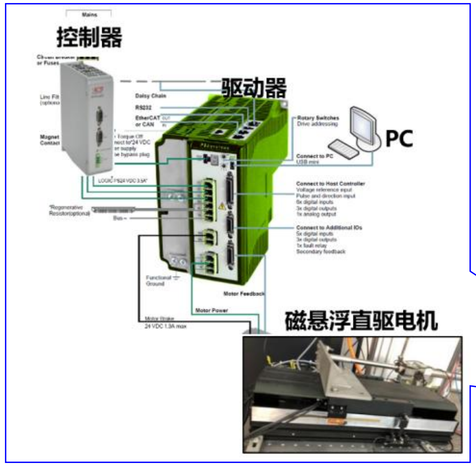

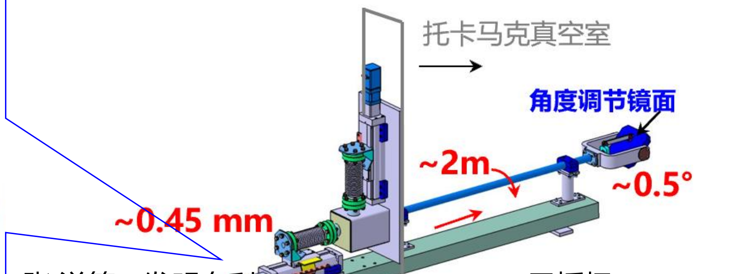

张洋等，发明专利ZL202110172094.0，已授权，2022.5

电子回旋波控制撕裂模实验研究

□ 传统理论认为，电子回旋波稳定撕裂模的主要机制是加热，改变整体电流密度分布

- 通过精细的实验方案设计，清晰观测到磁岛内部加热过程及其对磁岛宽度的影响（相位空间演化）
- 在MRE方程中加入ECRH加热致稳效应，更好地解释了实验观测结果；支持CLT模拟程序的发展

I_p ~ 400 kA, n_{e0} ~ 2.0×10^{19} m^{-3}, T_{e0} ~ 1.5 keV, B_{t0} ~ 2.2 T, q_{95} ~ 5, $\rho_{q=2}$ ~ 0.6

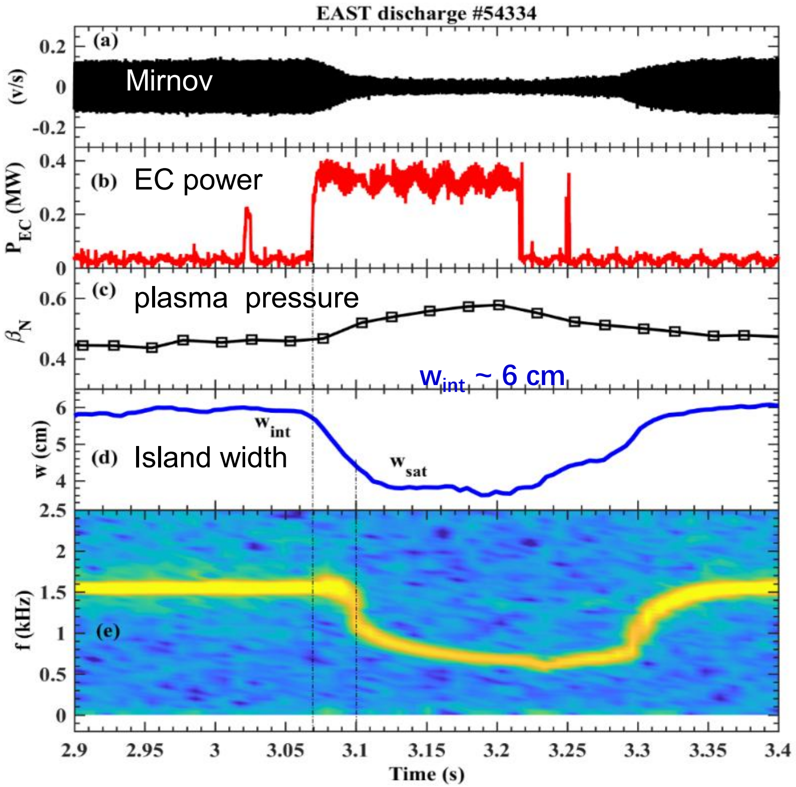

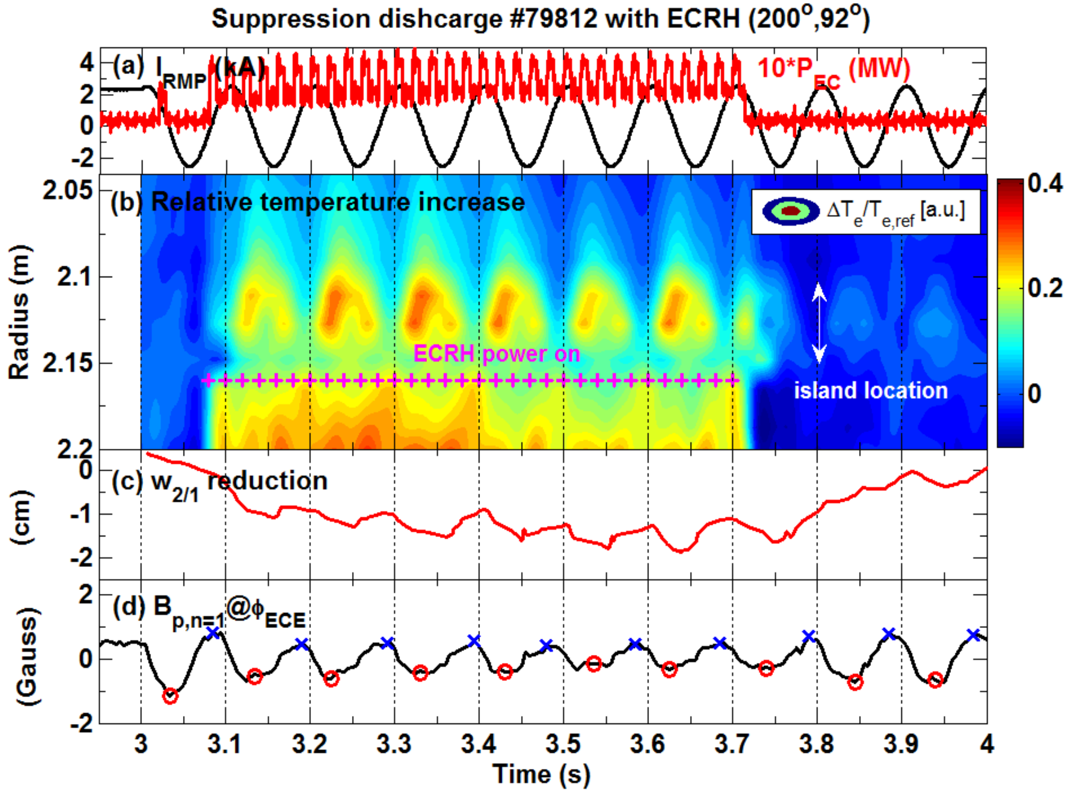

Y. Zhang, *et al*, *Nucl. Fusion* **61**, 096028 (2021)； W. Zhang, Z.W. Ma, Y. Zhang, *et al.*, AIP Advances **9**, 2019.

EAST装置首次实现新经典撕裂模的有效控制

□ EAST装置上利用RMP提供种子磁岛，主动激发NTM，成功实现电子回旋对NTM的有效抑制

- 明确EAST参数区间ECCD是稳定NTM的主要机制，但ECRH效应不可忽略，可允许的径向偏差 $\Delta\rho = \rho_{cd} - \rho_{2/1} < 0.03$
- 发现ELM与NTM的强相互作用，ECCD会加强相互作用

I_p = 500kA, B_t = 2.4 T, q_{95} ~ 5.0, T_{e0} = 2.5 keV, T_{i0} = 1.5 keV, n_{e0} = 3×10^{19} m^{-3}

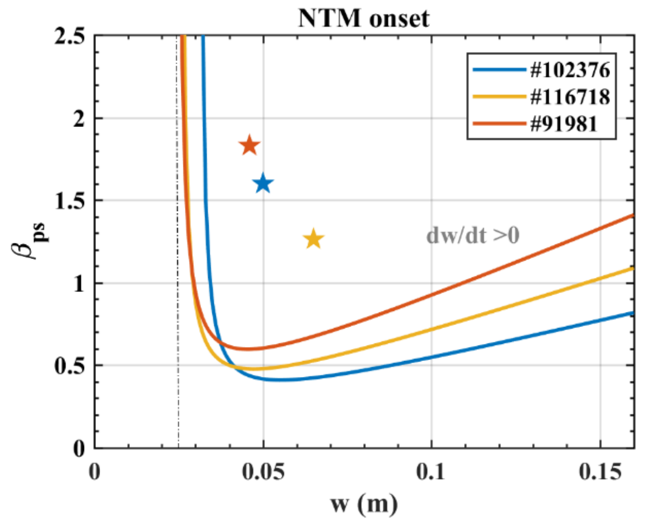

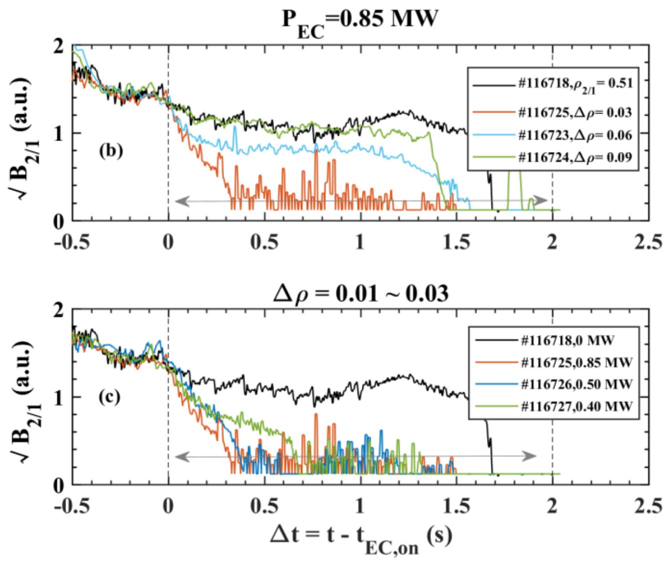

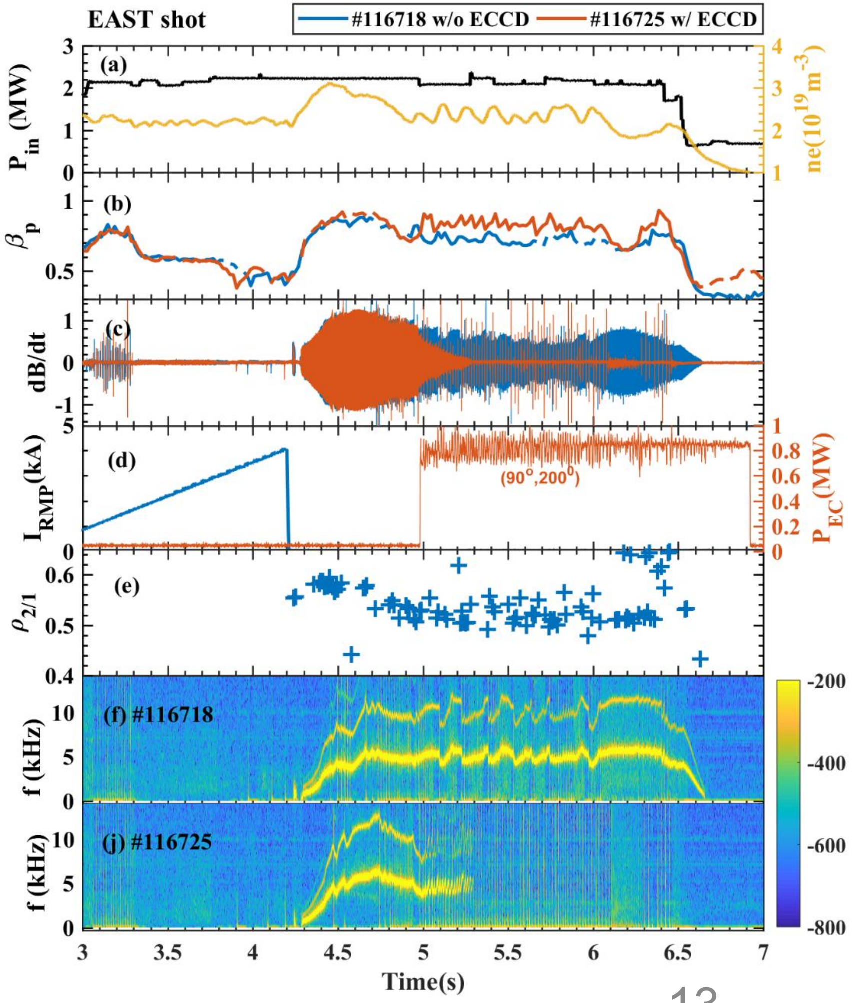

- ✓ Y. Zhang, *et al*, 23rd Workshop on MHD stability control, UCLA；
- ✓ Y. Zhang, *et al.*, 29th IAEA FEC, EX-S-2119, 16-21 Oct 2023

预先注入ECCD完全抑制NTM，避免锁模

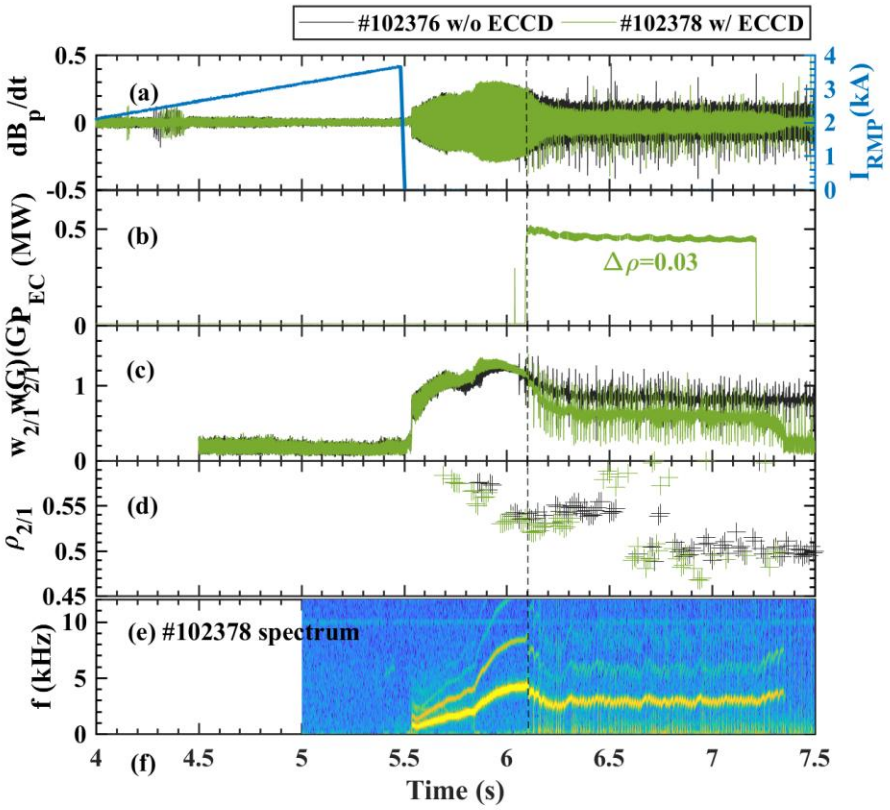

提前注入ECCD

并将磁岛O点锁定到ECCD相位

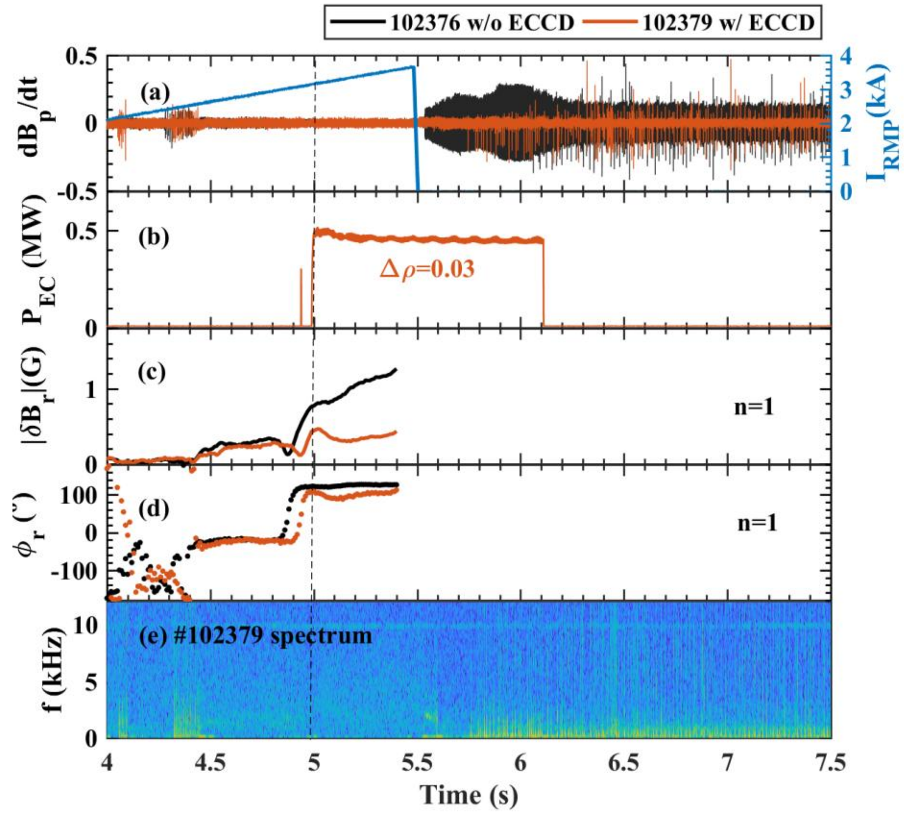

在磁岛饱和后投入ECCD@500kW，仅可实现部分抑制NTM

磁岛增长初始阶段提前投入ECCD@500kW，并与磁岛O点对齐，可以完全避免NTM出现

✓ Y. Zhang, *et al*, *Nucl. Fusion* **64** 076016 (2024)

电子回旋波控制撕裂模的数值模拟研究

- 发现在**低碰撞率**条件下，**快电子反常输运**会展宽电子回旋波的驱动电流密度分布， $w_{pt} \sim (\chi_{\perp f}/\nu_f)^{1/2}$ ，降低控制效果

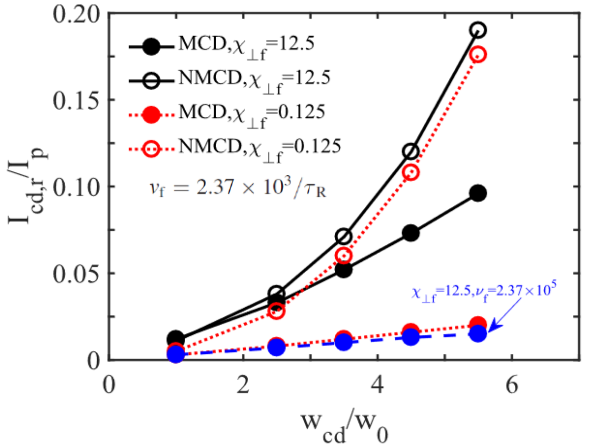

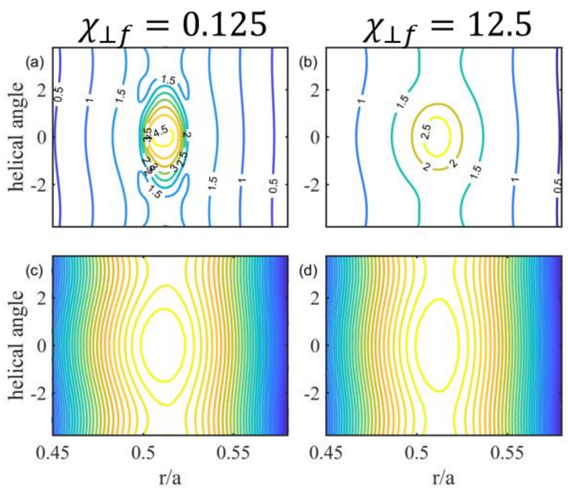

- 利用低于锁模阈值的RMP控制磁岛不均匀转动，可以提高控制效率

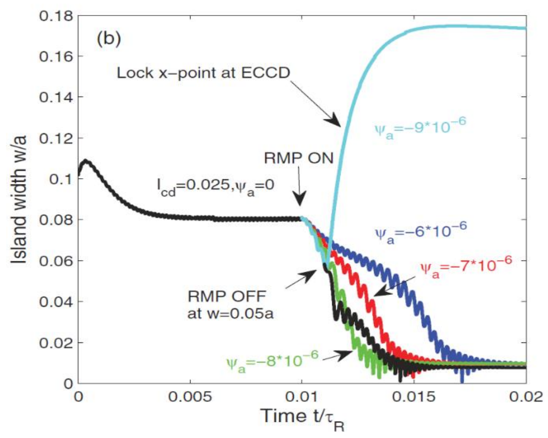

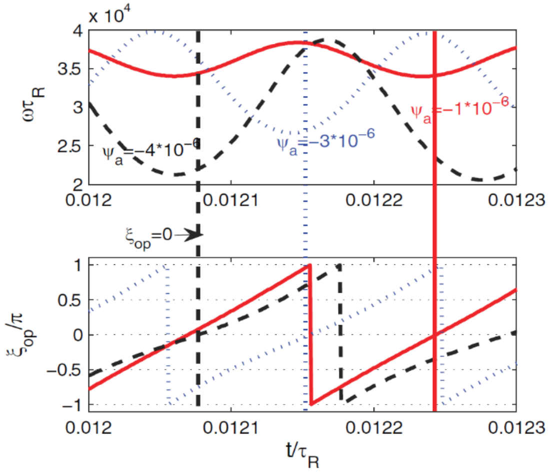

Reduce MHD code TM1 (by Q. Yu@ IPP)

- 采用柱位形，流体不可压（$\boldsymbol{v} = \nabla\emptyset \times \boldsymbol{e_t}$）
- 磁场 $\boldsymbol{B} = B_{0t}\boldsymbol{e_t} - (nr/mR)B_{0t}\boldsymbol{e_\theta} + \nabla\psi \times \boldsymbol{e_t}$
- 欧姆定律、等离子体涡旋方程和压力发展方程

$$\frac{\partial\psi}{\partial t} + \boldsymbol{v}\cdot\nabla\psi = E - \eta(j - j_b - j_{cd}),$$

$$\rho(\frac{\partial}{\partial t} + \boldsymbol{v}\cdot\nabla)\nabla^2\emptyset = \boldsymbol{e_t}\cdot(\nabla\psi \times \nabla j) + \rho\mu\nabla^4\emptyset,$$

$$\frac{3}{2}(\frac{\partial}{\partial t} + \boldsymbol{v}\cdot\nabla)p = \nabla\cdot(\chi_\parallel\nabla_\parallel p) + \nabla\cdot(\chi_\perp\nabla_\perp p) + Q$$

$$j = -\nabla^2\psi - 2nB_{0t}/(mR)$$

$$j_b = -c_b\frac{\sqrt{\varepsilon}}{B_\theta}\frac{\partial p}{\partial r}$$

- 快电子密度由二维输运方程来描述

$$\frac{\partial n_f}{\partial t} = \nabla\cdot(\chi_{\parallel f}\nabla_\parallel n_f) + \nabla\cdot(\chi_{\perp f}\nabla_\perp n_f) + \nu_f(n_{fs} - n_f)$$

- 快电子源$n_{fs} = n_{fs0}\exp\left[-\left(\frac{r-r_{cd}}{w_{cd}}\right)^2\right]\Pi(h_0, \Delta h)$
- $\Pi(h_0, \Delta h) = \begin{cases} 1, & |h - h_0| < \Delta h \\ 0, & \text{其它} \end{cases}$

X.J. Wang, Y. Zhang*, *et al*, *NF* **62** 066007 (2022)；X.G.Wang, X.D. Zhang, Q,Yu, Y. Zhang, NF **55** (2015) 093024

报告提纲

- □ 背景介绍
- □ EAST新经典撕裂模控制研究
  - ➢ 控制技术、实验研究、模拟计算
- □ **AI带来的变革与突破**

当前新经典撕裂模研究面临的挑战

- ☐ 如何提高NTM的控制效率，降低功率需求？
- ☐ 寻找物理和技术的平衡点，探索适用于反应堆的高效方法

• 发展新方法，利用弹丸注入（湍流），提高ECCD控制NTM的效率

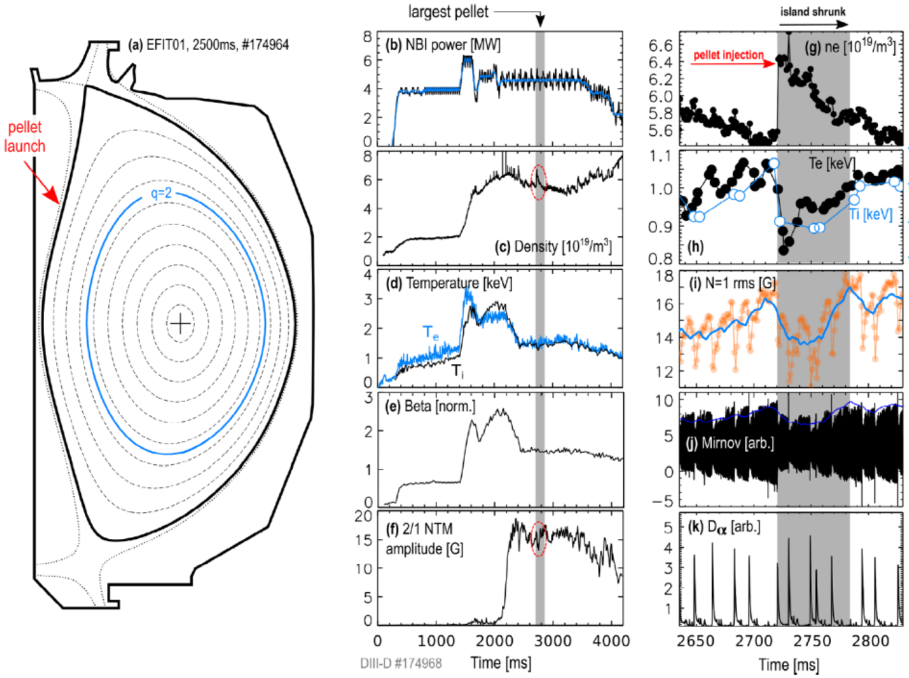

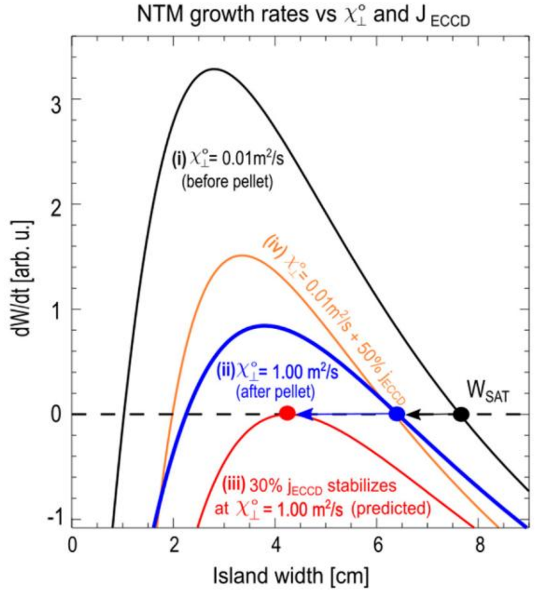

L. Bardoczi, et al., Nucl. Fusion **59** (2019)

• 优化控制技术，降低探测精度需求

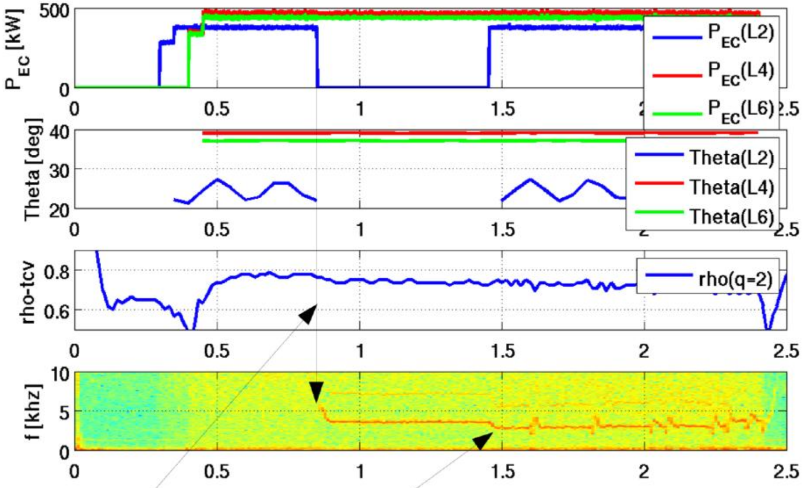

F. Felicia, NF 52 074001; D. Kim,PhD Thesis 2015

• 利用协同作用：LHW + ECCD

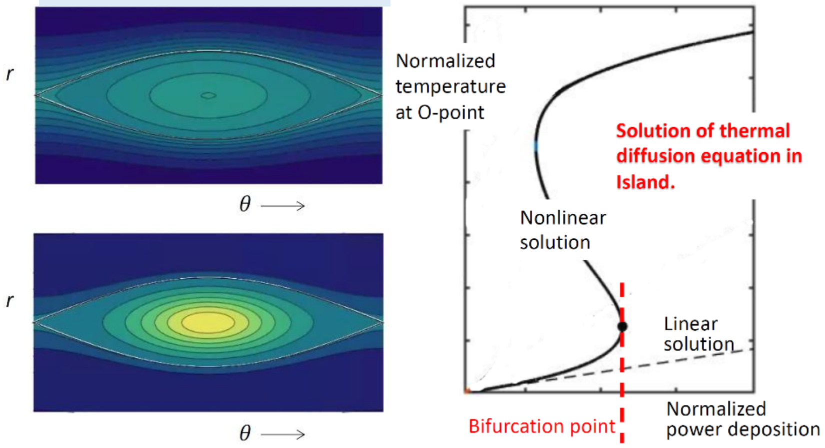

A. Reiman and N. Fisch, PRL **121**, 225001 (2018).

成功避免的新经典撕裂模的出现

- **基于强化学习的人工智能（DNN）：**
  - **Observation:** plasma state (shape profiles) → Dynamic model for tearing-instability prediction
  - **Action**: Beam power, ECRH, PF coil current
  - **Reward:** Fusion Gain, no Tearing instability

$$R(\beta_N, T; k) = \begin{cases} \beta_N, & \text{if } T < k \\ k - T, & \text{otherwise} \end{cases}$$

Constrain q_{95} and plasma rotation to maintain ITER baseline-similar condition

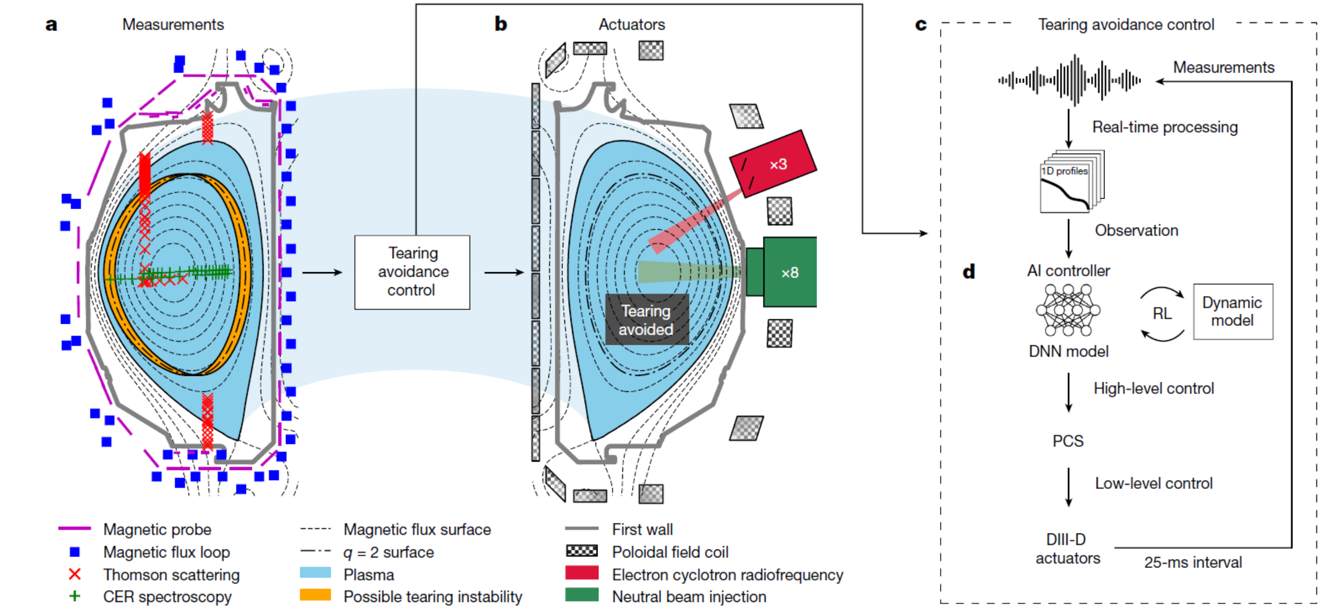

Fig. 1 | The overall architecture of the tearing-avoidance system in the DIII-D tokamak. a, The selected diagnostic systems used in this work: magnetics, Thomson scattering (TS) and charge-exchange recombination (CER) spectroscopy. The possible tearing instability of $m/n = 2/1$ is shown in orange. **b**, The heating, current drive and control actuators used in this work. **c**, Schematic description of the tearing-avoidance control, including preprocessing, high-level control by a DNN and low-level control by a PCS. **d**, The AI controller based on the DNN.

✓ J. Seo, et al., *Nature* 626 (2024) 747

ASIPP

亮点1：动理学分布的实时重构

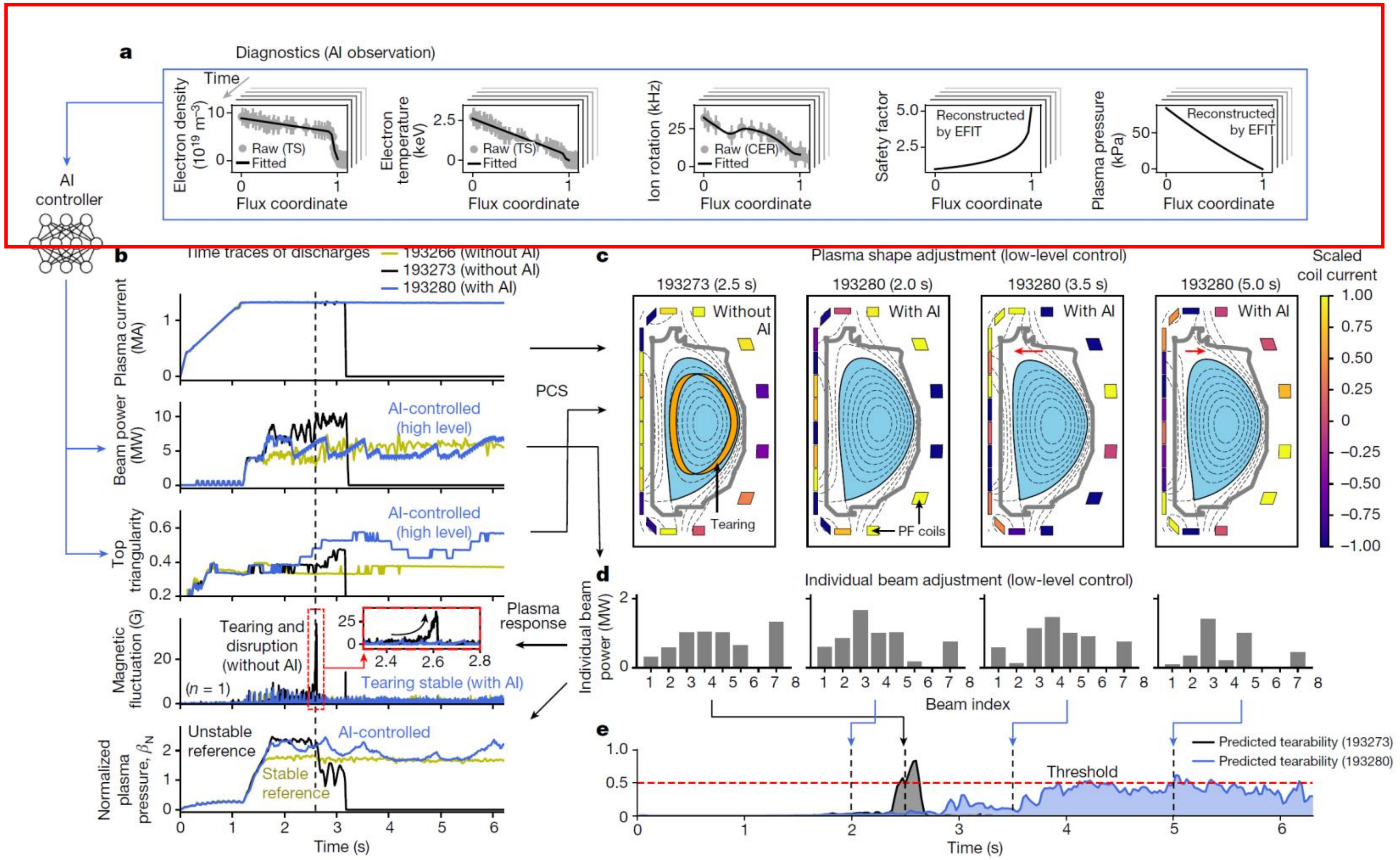

Fig. 3 | The AI-based tearing-avoidance experiments in DIII-D. a, The observation of the AI controller; the preprocessed profiles of electron density, electron temperature, ion rotation, safety factor and plasma pressure. **b**, The time traces of discharges 193266 (stable reference), 193273 (unstable reference) and 193280. Discharge 193280 is the AI-controlled one. **c**, The low-level coil current control by the PCS and the plasma boundary variation. Scaled currents of poloidal field (PF) coils are shown in colour. **d**, The low-level individual beam power control by the PCS. **e**, The estimated tearability for discharges 193273 and 193280.

实时动理学分布重构，自洽地给出等离子体电子密度分布、温度分布、电流分布、旋转分布、和压强分布

动理学分布是评估撕裂模稳定性的关键参数

Real-time plasma profiles observation (t)

Data-driven model

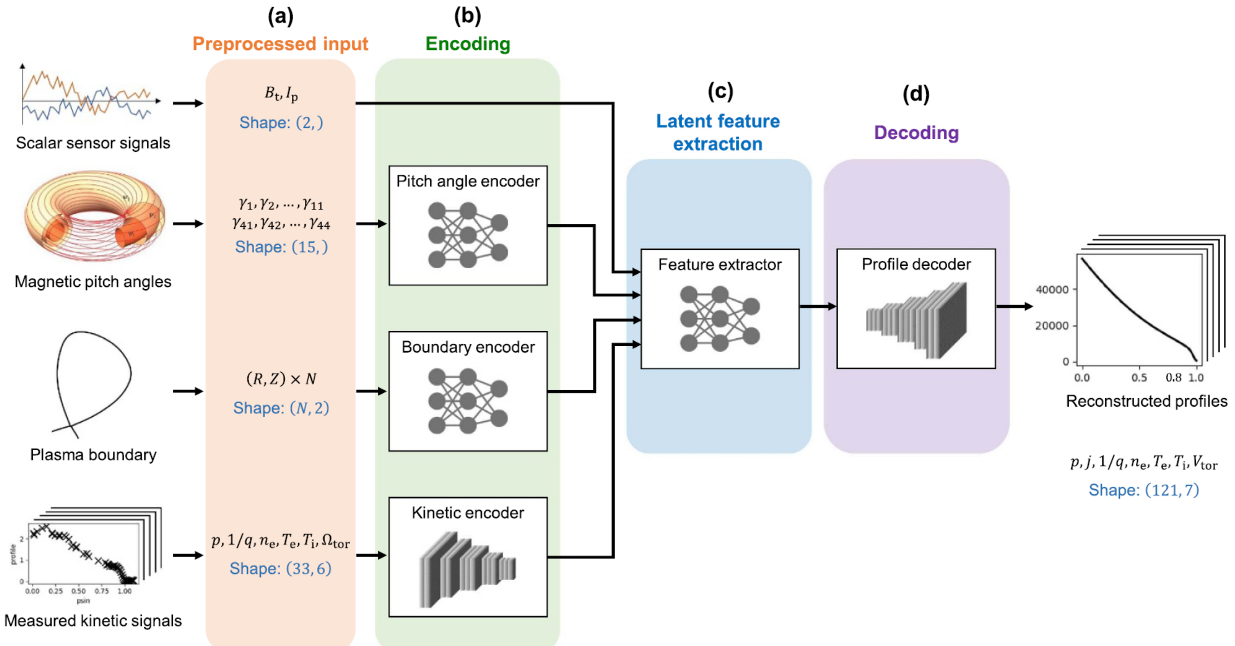

Figure 1. Neural network architecture for multimodal prediction of kinetic equilibrium profiles.

CAKE: Consistent Automatic Kinetic Equilibrium reconstruction

RTCAKENN: ML based real-time kinetic profile reconstruction

- ✓ R.Shousha, et al., *Nucl. Fusion* 64 (2024) 026006
- ✓ Z.A. Xing, et al., *Fusion Eng. Design* 163 (2021) 112163

Physics-based model

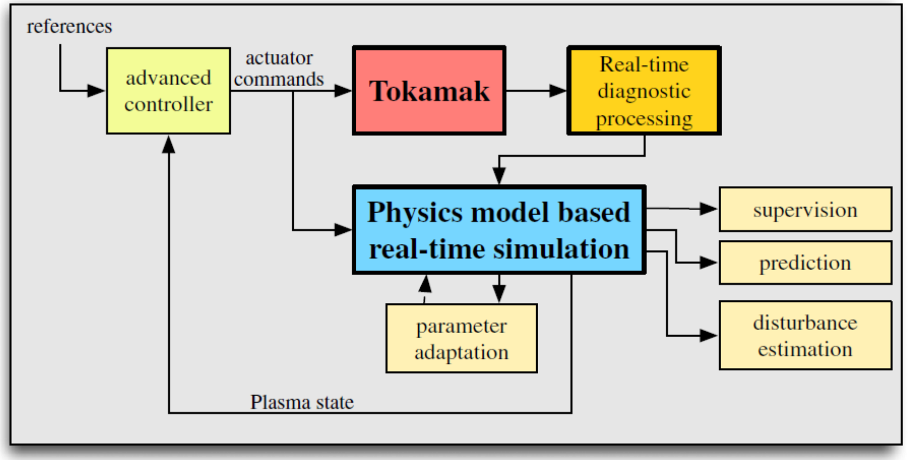

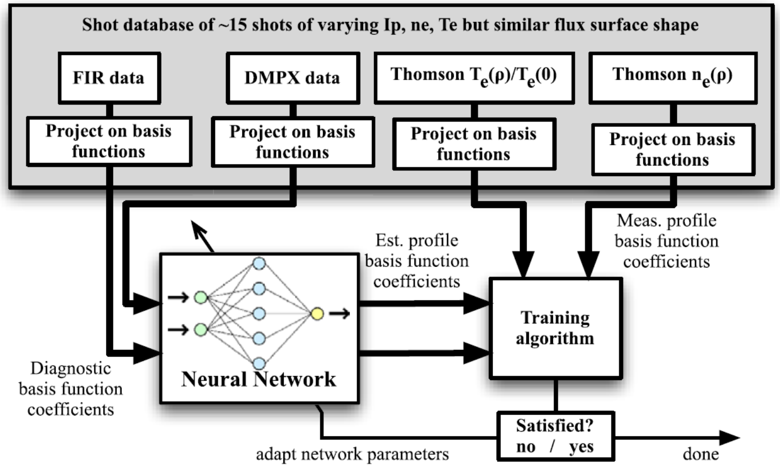

- ✓ F. Felici *et al* 2011 *Nucl. Fusion* **51** 083052

Real-time plasma profiles prediction (t+Δt)

- **Approximate the profile (t + Δt) from given**
  - **1D profiles (t)**
  - **0D plasma parameters (t)**
  - **actuator settings (t + Δt)**

Data-driven model

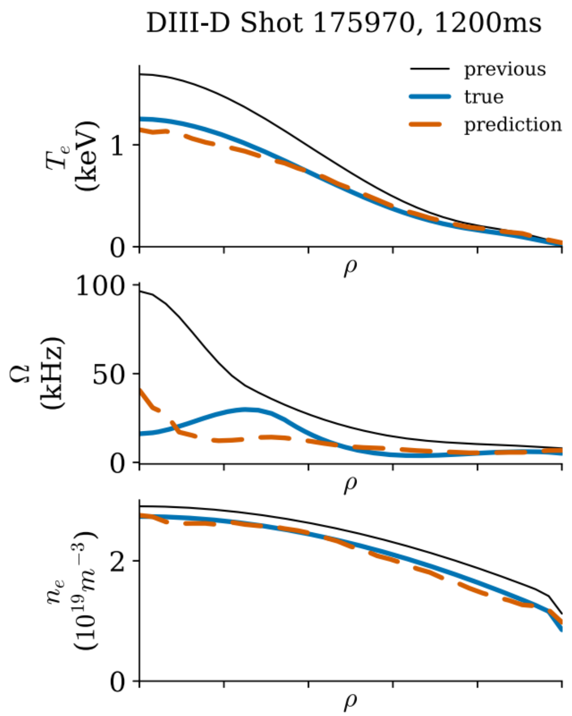

$$\frac{\mathrm{d}\boldsymbol{x}}{\mathrm{d}t} = \boldsymbol{f}(\boldsymbol{x}, \boldsymbol{u}),$$

$$\boldsymbol{x}_{t+1} = \boldsymbol{x}_t + \boldsymbol{f}(\boldsymbol{x}_t, \boldsymbol{u}_t),$$

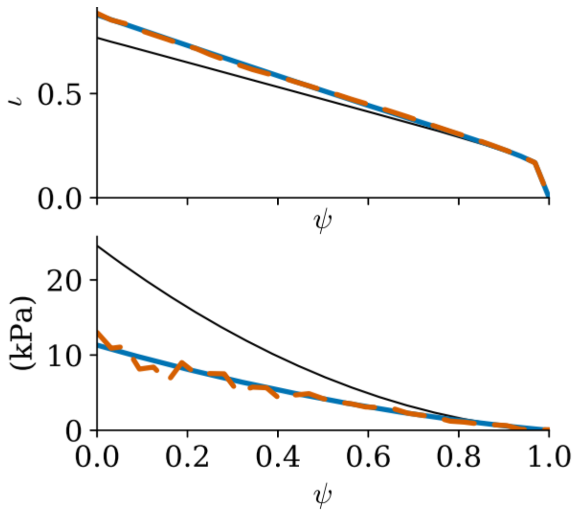

✓ J. Abbate, et al., Nuclear Fusion 61 (2021) 046027.

- **JETTO** transport code has been used to predict T_e, T_i, n_e, and rotation on JET scenarios
- **TRANSP** has been used to predict Te and Ti on DIII-D scenarios with GLF23 or TGLF to calculate transport coefficients, and NUBEAM for beam deposition
- **OMFIT's STEP** workflow seeks consistency among these quantities via core-pedestal and impurity transport coupling.

Predictive simulation codes

亮点2：撕裂模不稳定性的预测

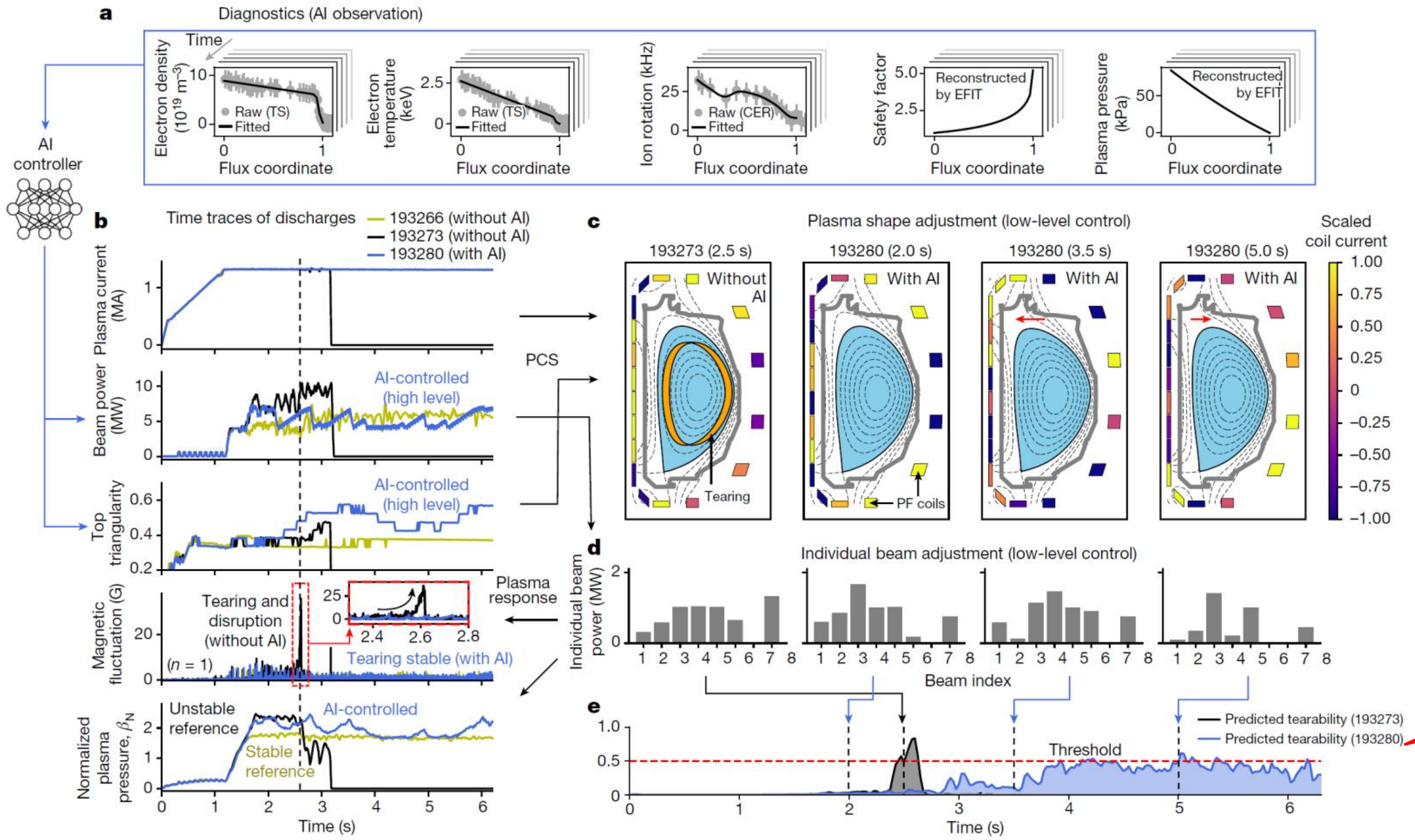

Fig. 3 | The AI-based tearing-avoidance experiments in DIII-D. a, The observation of the AI controller; the preprocessed profiles of electron density, electron temperature, ion rotation, safety factor and plasma pressure. **b**, The time traces of discharges 193266 (stable reference), 193273 (unstable reference) and 193280. Discharge 193280 is the AI-controlled one. **c**, The low-level coil current control by the PCS and the plasma boundary variation. Scaled currents of poloidal field (PF) coils are shown in colour. **d**, The low-level individual beam power control by the PCS. **e**, The estimated tearability for discharges 193273 and 193280.

利用当前时刻的动理学分布参数（t），结合actuator（t+ Δt ）的建议参数，预测处（t+Δt）撕裂模不稳定性

Tearability prediction

Dynamic model for tearing-instability prediction

☐ A DNN-based multimodal dynamic model, integrated with openAI

- **Input:** ($n_e(r)$, $T_e(r)$, $T_i(r)$, $V_t(r)$, q(r)…) + actuations (Bt, Ip,….)
- **Output:** the 25-ms-after tearing likelihood to be predicted

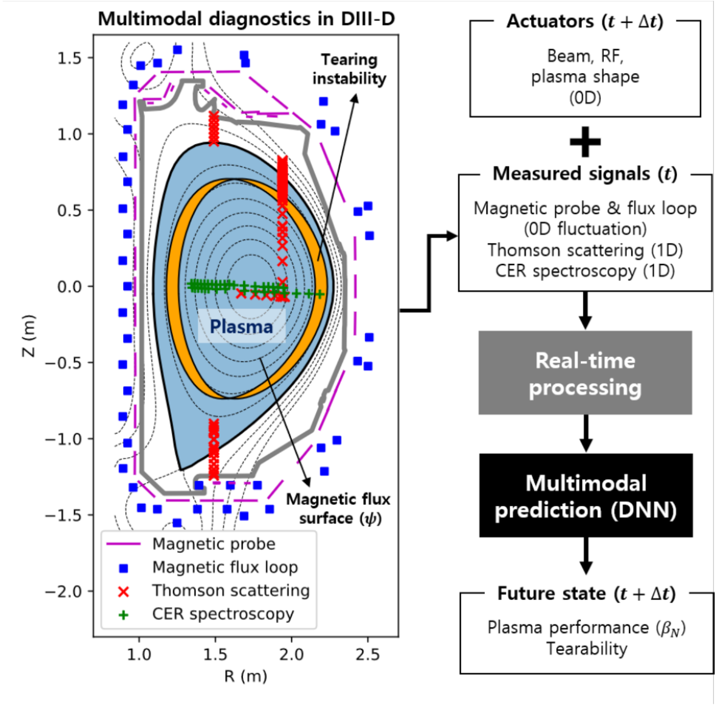

Fig. 1. The diagram of the proposed tearing instability prediction model and the selected diagnostics of DIII-D tokamak that are used as inputs to the model. A possible tearing instability of $m = 2$ and $n = 1$ is illustrated with an orange shade.

A black box used as a **surrogate** for the response of stability

to predict β_N and tearability at t + Δt by looking at the plasma profile signals at time *t* as well as "suggested" actuators values for t + Δt

The data-driven DNN model could cover the complicated physics of the interaction among the rotation, current profile, and tearing instability

vs 锁模预测?

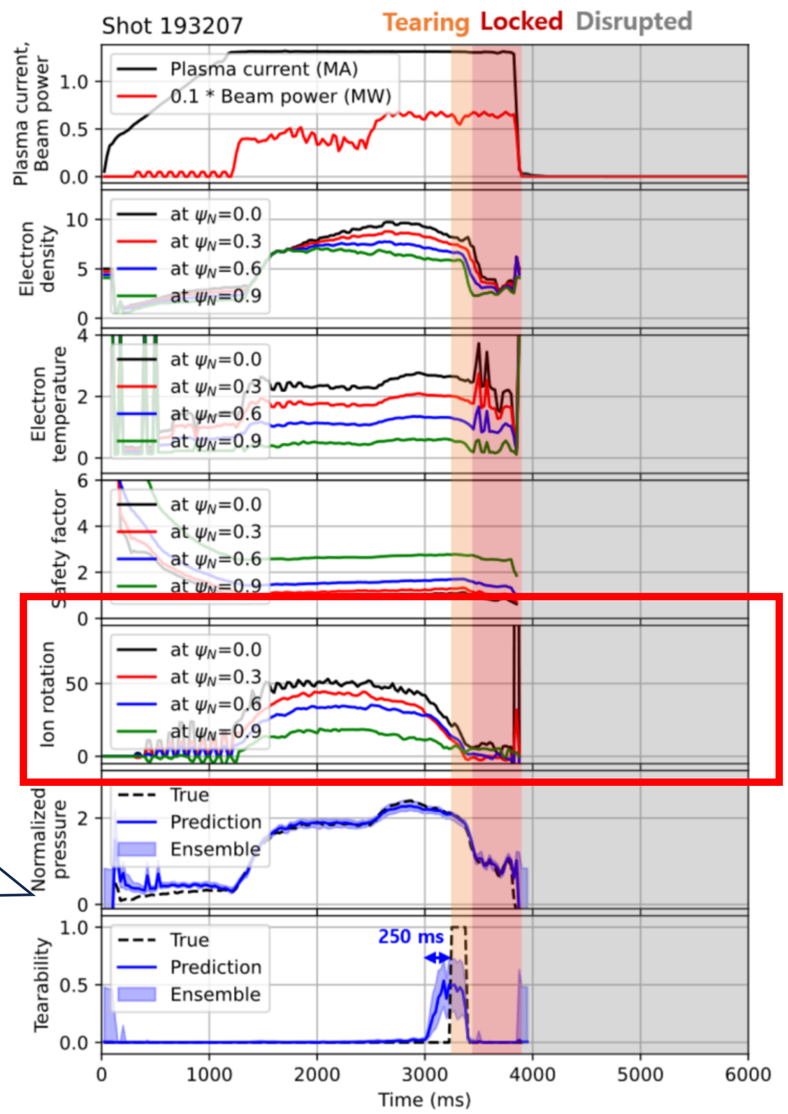

✓ J. Seo, *et al.*, Multimodal prediction of tearing instabilities in a tokamak. In *2023 IJCNN* 1–8 (IEEE).

Develop an operation trajectory design algorithm

□ AI 控制成功实现了避障，发现了高G存在的一个低 Tearability 山谷

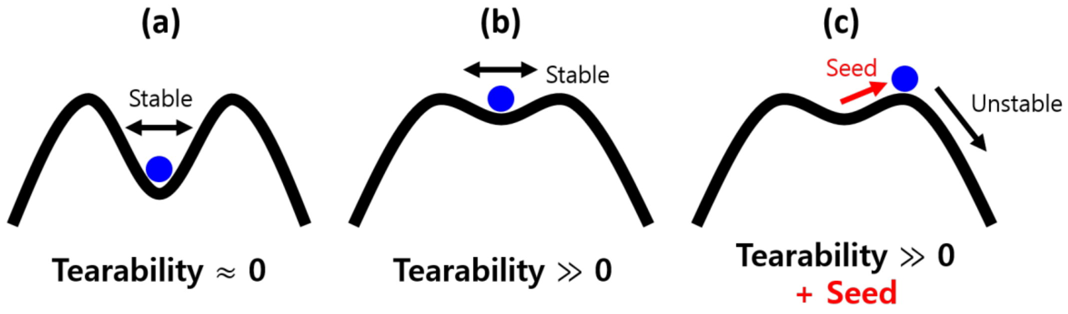

tearing instability is nearly stochastic even after the tearability increases

“常在河边走，就是不湿鞋”

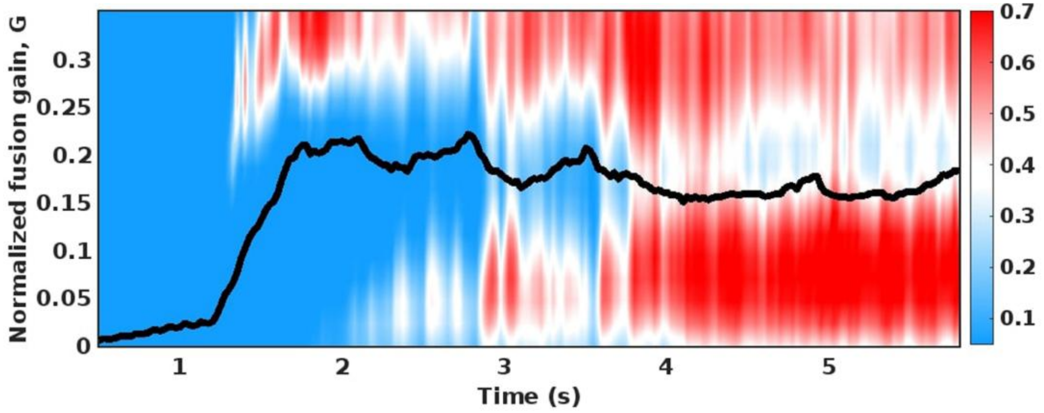

Extended Data Fig. 6 | Time trace of the normalized fusion gain for discharge 193280, where contour color illustrates the tearability. The RL control successfully drives plasma through the valley of tearability.

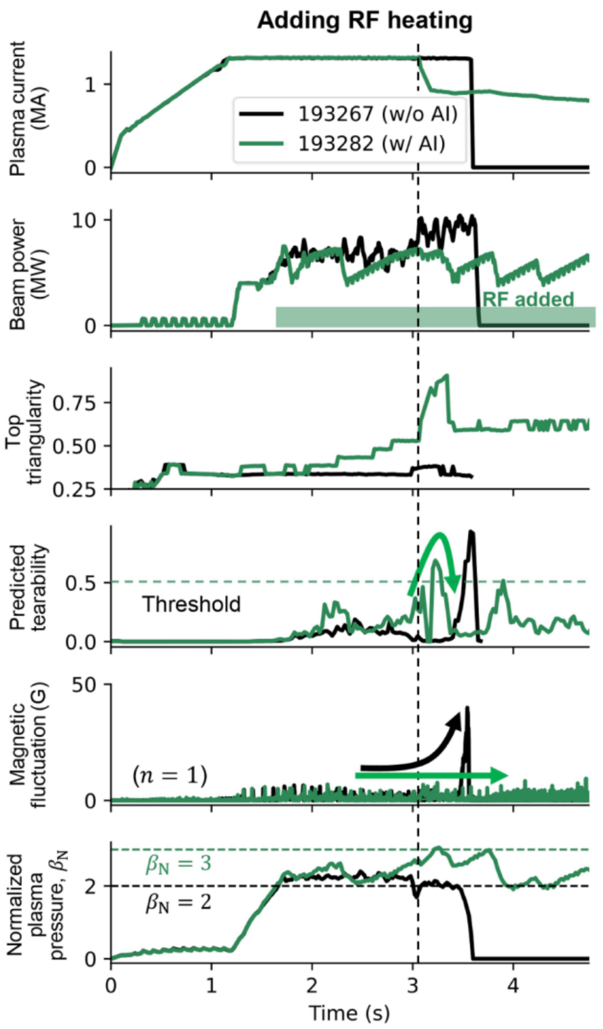

Extended Data Fig. 8 | Control experiments under the different plasma conditions by adding RF heating. In the AI-controlled discharge (193282), the plasma current control is suddenly lost at $t = 3.1$ s, but the tearability control is still working after that.

J. Seo, et al, *Nucl. Fusion* **61** (2021) 106010; J. Seo, et al, *NF* **62** (2022) 086049

亮点3：撕裂模控制无需电子回旋波

High level

总束功率

三角度

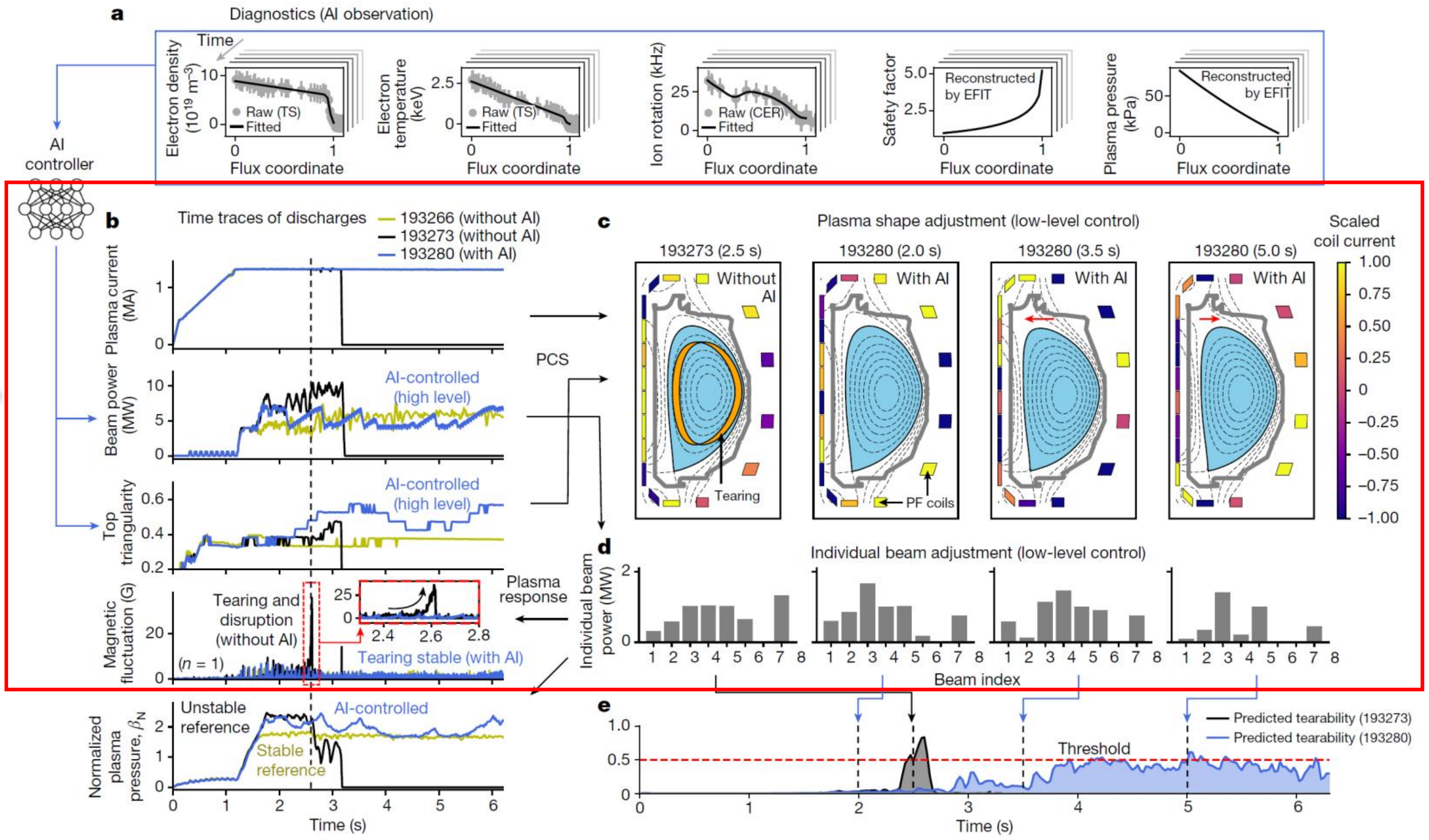

Lower level

PF电流

单支束功率

Fig. 3 | The AI-based tearing-avoidance experiments in DIII-D. a, The observation of the AI controller; the preprocessed profiles of electron density, electron temperature, ion rotation, safety factor and plasma pressure. **b**, The time traces of discharges 193266 (stable reference), 193273 (unstable reference) and 193280. Discharge 193280 is the AI-controlled one. **c**, The low-level coil current control by the PCS and the plasma boundary variation. Scaled currents of poloidal field (PF) coils are shown in colour. **d**, The low-level individual beam power control by the PCS. **e**, The estimated tearability for discharges 193273 and 193280.

AI Controller based on another DNN model

- The tearing-avoidance controller, another DNN model, is trained using the deep deterministic policy gradient method, which is implemented using Keras-RL (https://keras.io/).

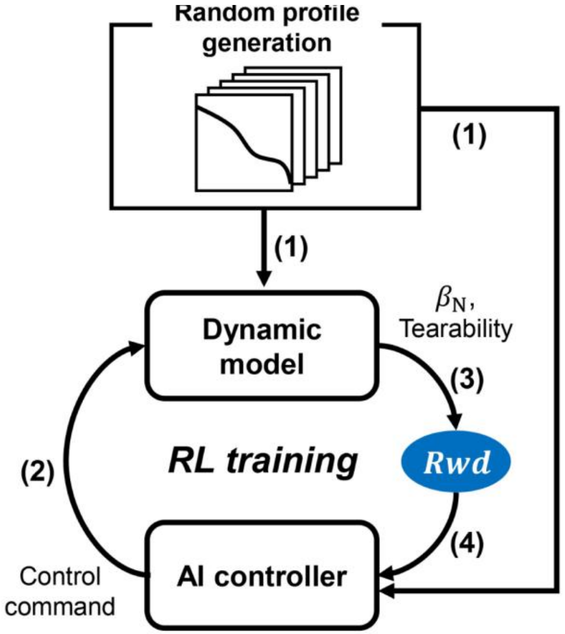

Extended Data Fig. 4 | The pipeline of the RL training used in our work. First, random plasma profiles are selected from experimental data to be fed to both the dynamic model and the AI controller. The AI controller observes the plasma profiles and determines the action. Then, the dynamic model predicts the future β_N and tearability. Lastly, the reward is estimated from the predicted state to optimize the AI controller.

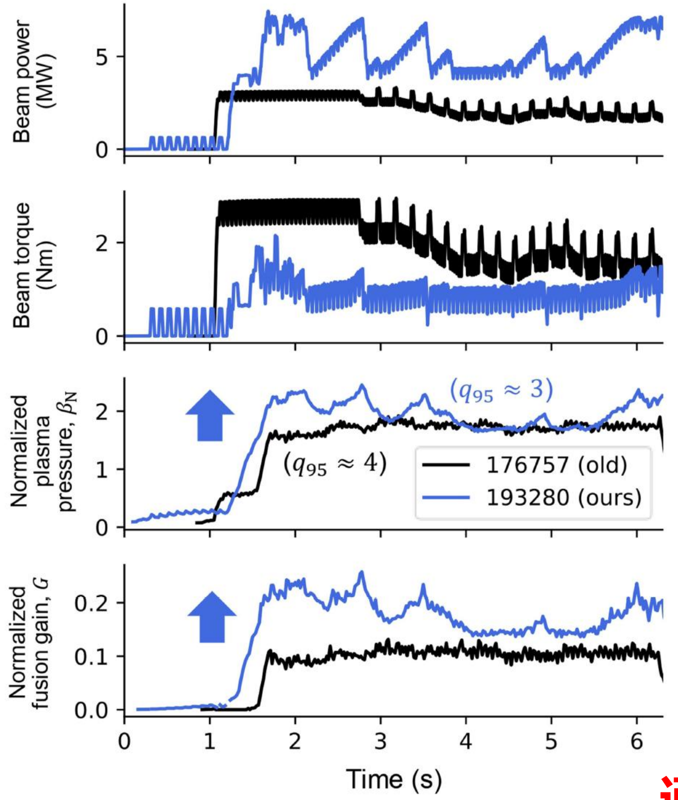

→ 高NB功率

→ 低动量

→ 高比压，低q

→ 高G $G \propto \beta_N/q_{95}^2$

Extended Data Fig. 5 | Comparison of the discharge using a previous controller (176757) and our controlled one (193280). Multi-actuator multi-objectives control could achieve higher β_N and G under more unfavorable condition. Here, the time domain for 176757 was shifted by +0.75 s to synchronize the H-mode onset between two shots.

Old: **bang-bang control scheme** using only beam power to handle tearability.

通过优化控制算法，提高了等离子体性能，同时避免NTM

Y. Fu, et al. *Phys. Plasmas* 27, 022501 (2020).

小 结

- AI技术的引入，为解决撕裂模不稳定性这一托卡马克等离子体重大科学问题提供了全新的解决方案
- 通过调节旋转（beam power）和位形（PF coils）来，来调控宏观kinetic profiles，以避免局域Tearing instability；

  背后对应的可能物理机理： 旋转 → 极化电流；位形 → current profiles
- Tearability prediction基于1D分布参数和actuators下一步动作命令，预测Tearing instability，但无法预测触发NTM的seeds → 存在潜在的不确定性
- 本质上没有突破物理极限，而是在接近物理极限的边缘，利用AI实现了优于传统控制方法的复杂问题的精细决策， 获得更高β_N，低q95，低动量，高聚变增益
- 高质量的实验数据库的发展与积累，为AI模型的发展提供了非常重要的基础

小 结

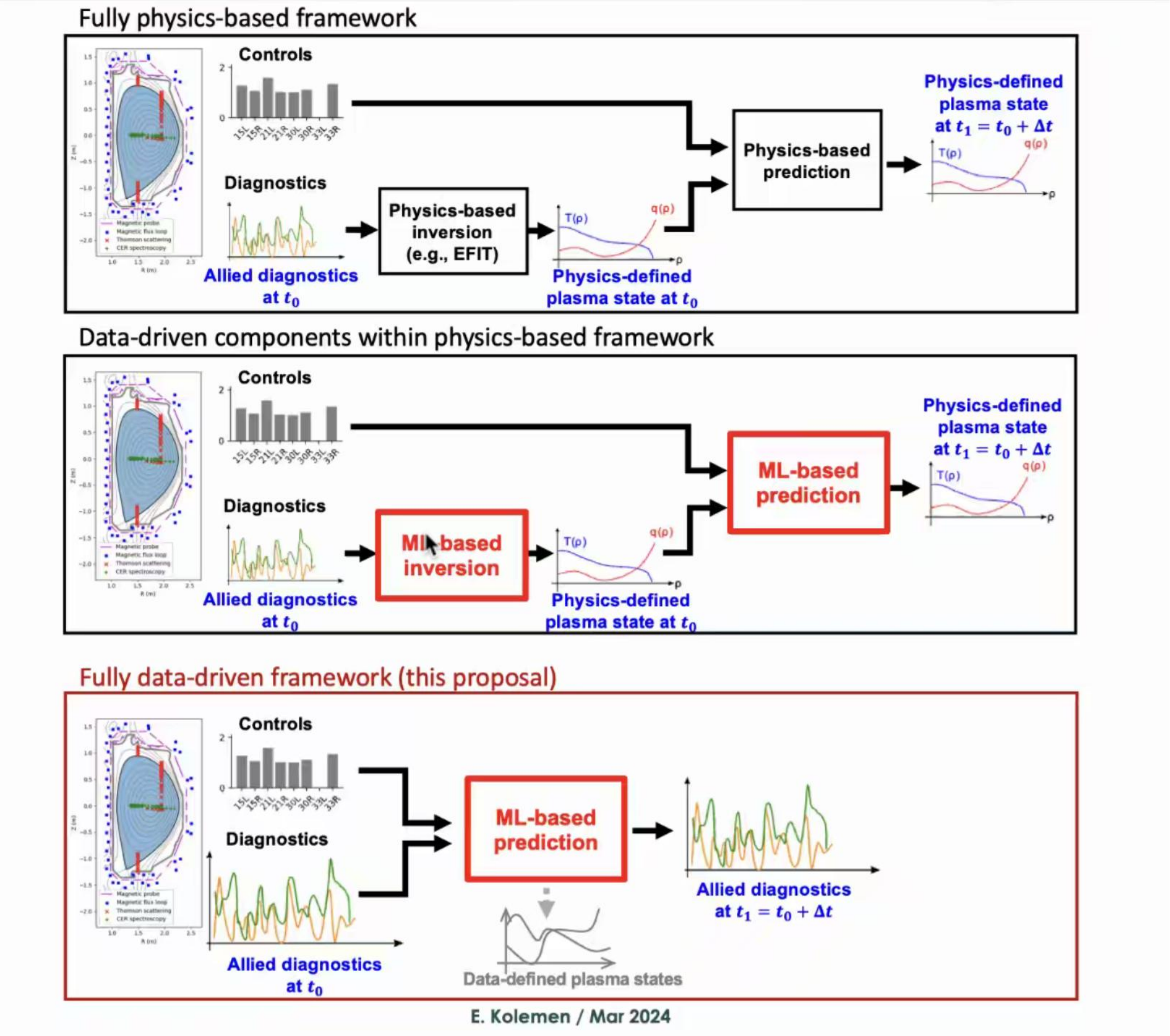

- ✓ F. Felici *et al* 2011 *Nucl. Fusion* **51** 083052
- ✓ Z.A. Xing, et al., *Fusion Eng. Design* 163 (2021) 112163
- ✓ J. Abbate, et al., Nuclear Fusion 61 (2021) 046027
- ✓ J.T. Wai, Neural net modeling of equilibria in NSTX-U, *Nucl.Fusion* 62 (2022) 086042
- ✓ J. Seo, et al, *Nucl. Fusion* **62** (2022) 086049
- ✓ J. Seo, et al, *Nucl. Fusion* **61** (2021) 106010
- ✓ J. Seo, *et al*., Multimodal prediction of tearing instabilities in a tokamak. In *2023 International Joint Conference on Neural Networks (IJCNN)* 1–8 (IEEE, 2023).
- ✓ J. Seo, *et al., Nature* 626 (2024) 747